Received February 2000
Revised September 2000
Accepted September
2000

Global numerical prediction of bursting frequency in turbulent boundary layers

William W. Liou, Yichuan Fang
Department of Mechanical and Aeronatical Engineering, Western Michigan University, Kalamazoo, USA and
Roy S. Baty
Sandia National Laboratories, Albuquerque, USA

Keywords *Turbulence, Numerical methods, Eigenvalues, Boundary layers*

Abstract *The frequencies of the bursting events associated with the streamwise coherent structures of spatially developing incompressible turbulent boundary layers were predicted. The structures were modeled as wavelike disturbances associated with the turbulent mean flow using a direct-resonance theory. Global numerical solutions for the resonant eigenmodes of the Orr-Sommerfeld and the vertical vorticity equations were developed. The global method involves the use of second and fourth order accurate finite difference formulae for the differential equations as well as the boundary conditions. The predicted resonance frequencies were found to agree very well with previous results using a local shooting technique and measured data.*

Nomenclature

A_v	=	coefficient in equation (7)
B_v	=	coefficient in equation (7)
B_η	=	coefficient in equation (8)
$\mathbf{C}$	=	coefficient matrices in equation (10)
D	=	$\frac{d}{dy}$
$\mathbf{D}$	=	lambda matrix
F_i	=	averaged turbulence quantity
L	=	length scale
Re	=	Reynolds number
U	=	mean velocity in the x-direction
c	=	wavespeed
i	=	index or $\sqrt{-1}$
m	=	transformation metric $\frac{d\bar{y}}{dy}$
t	=	time
x	=	x coordinate
y	=	y coordinate
z	=	z coordinate
U_∞	=	free stream velocity
$\bar{f}_i$	=	turbulence quantity
f_i'	=	background fluctuation
$\tilde{f}_i$	=	wavelike component
u_τ	=	wall frictional velocity
$\hat{v}$	=	mode shape for the wavelike y–component of velocity
$\mathbf{v}$	=	solution vector in equation (9)
$\bar{y}$	=	transformed y coordinate
y^+	=	$\frac{yu_\tau}{\nu}$
α	=	wavenumber in the x-direction
β	=	wavenumber in the z-direction
δ	=	boundary layer thickness
δ^*	=	boundary layer displacement thickness
$\hat{\eta}$	=	mode shape for the x-component of vorticity
ν	=	kinematic viscosity
ω	=	frequency
ω^+	=	$\frac{\omega\nu}{u_\tau^2}$

The work was supported by Sandia National Laboratories, USA. The technical monitor was Dr Roy S. Baty.

Introduction

Many experimental results on incompressible and compressible turbulent boundary layers have indicated the existence of coherent structures in such flows. The quasi-deterministic occurrence of large-scale organized structures is collectively called the bursting process. A sketch of the bursting event (Cantwell, 1989) is shown in Figure 1. The bursting process is believed to play a dominant role in the development of turbulent boundary layers.

The bursting process is associated with the appearance of counter-rotating vortex structures. Experiments by Morrison and Kronauer (1969) showed that the statistically dominant streamwise fluctuations exhibited wavelike characteristics, suggesting that a hydrodynamic wave description for the streamwise structures is applicable.

Based on a weakly nonlinear theory, Jang *et al.* (1986) proposed that resonance could occur for certain damped three-dimensional modes when the eigenmodes of the Orr-Sommerfeld solution corresponded to that associated with the vertical vorticity equation. They showed that for incompressible turbulent boundary layers, the secondary mean flow induced by these resonant fundamental modes contained streamwise vortical structures.The shape of the predicted structures and the spacing of the accompanying low-speed streaks are comparable with experimental observation.

Because of the nature of the numerical integration scheme used in Jang *et al.* (1986), some knowledge of the eigenvalues is required a priori in order for the numerical solution to be successful. Since this information is not readily

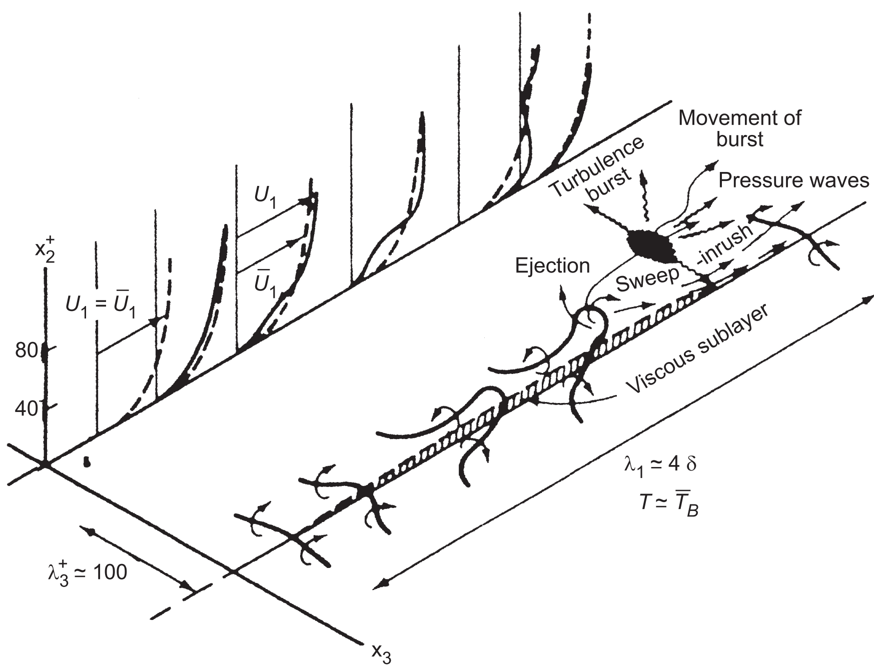

Figure 1.
A sketch of the bursting event (Cantwell, 1989)

available beyond a few simple profiles for the mean quantities, it severely limits the use of the direct-resonance method in simple flow cases. Furthermore, the eigenvalue spectra of the Orr-Sommerfeld and the vertical vorticity equations contain many other eigenmodes. It is possible that the eigenmodes not considered in Jang *et al.* (1986) might also excite resonance. These issues may become a major concern when the flow speed increases, and effects of compressibility are included.

In addition, the Orr-Sommerfeld and the vertical vorticity equations yield stiff systems of ordinary differential equations. In the process of the numerical integration of a stiff system, numerical errors associated with one solution may contaminate the other and lose their linear independence. Extra care, such as the use of a re-orthonormalization procedure, is required to keep the solution independent. In this study we implemented a modern global numerical scheme for the eigenvalue problems. A global method solves the equations using a global approximation of the solution. The global solution method does not require a re-orthonormalization procedure and is ideal for stiff systems, such as the Orr-Sommerfeld and the vorticity equations (Liou and Morris, 1992a; Baty and Morris, 1995; Bridges and Morris, 1984).

The global method provides a description of the entire eigenvalue spectrum of the stability problem without using any prior knowledge of the eigenvalues, as is required by the traditional shooting procedure. As such, all possible bursting frequencies are likely to be identified automatically without artificial intervention. This capability allows an efficient numerical prediction of bursting frequencies.

In this study second – and fourth – order accurate finite difference formulae have been used in approximating the incompressible Orr-Sommerfeld equation, the vertical vorticity equation, and their boundary conditions.

In the following, the derivation and the solution of the equations are described. The results are presented in the last section.

Modeling

Turbulence quantities, $\overline{f_i}$, are decomposed into three components (Liou and Morris, 1992b):

$$\overline{f_i} = F_i + f_i + f_i', \tag{1}$$

where F_i represents a long-time average of $\overline{f_i}$, f_i the wave like component of $\overline{f_i}$, and f_i' the background fluctuation. Substituting equation (1) into the Navier-Stokes equations, followed by a linearization of the disturbance quantities, the equations governing the mode shape of the vertical velocity, $\hat{v}$, the Orr-Sommerfeld equation, and the homogeneous vertical vorticity, $\hat{\eta}$, equation can be found:

$$\left[\mathrm{i}(\alpha U - \omega)(D^2 - \alpha^2 - \beta^2) - \mathrm{i}\alpha D^2 U - \frac{1}{Re}(D^2 - \alpha^2 - \beta^2)^2\right]\hat{v} = 0 \tag{2}$$

$$\left[\mathrm{i}(\alpha U - \omega) - \frac{1}{Re}(D^2 - \alpha^2 - \beta^2)\right]\hat{\eta} = 0 \quad (3)$$

Equations (2) and (3) have been derived by assuming a normal mode solution for the wavelike disturbances, f_i, i.e.

$$f_i = \hat{f}_i \mathrm{e}^{\mathrm{i}(\alpha x + \beta z - \omega t)}. \quad (4)$$

In equations (2) and (3), U represents the streamwise mean velocity, and $D \equiv \mathrm{d}/\mathrm{d}y$. Equations (2) and (3) govern the mode shape of wavelike disturbances associated with the mean quantities in terms of the streamwise and spanwise wave numbers, α and β; the wave frequency, ω; and the flow Reynolds number, $Re(= \frac{U_\infty L}{\nu})$. In this study the bursting frequencies of the streamwise coherent structures in turbulent boundary layers are sought using the direct-resonance model. The condition for direct resonance can be written as

$$c^{OS}(\alpha, \beta, Re) = c^{VV}(\alpha, \beta, Re) \quad (5)$$

where c^{OS} and c^{VV} represent the phase velocity, ω/α, associated with the Orr-Sommerfeld and the vertical vorticity eigenvalue problems respectively.

The boundary conditions for $\hat{v}$ and $\hat{\eta}$ are

$$\hat{v} = D\hat{v} = \hat{\eta} = 0 \quad \text{at} \quad y = 0,\ \infty. \quad (6)$$

In the following section the numerical solution of equations (2), (3), (5), and (6) are described.

Numerical solutions

Mean flow

In contrast to the laminar stability calculations, the Blasius-type of solution can not be used to describe the mean flow velocity in the present study. The local turbulent mean velocity in the streamwise direction, U, needed for the current incompressible turbulent flat-plate boundary layers can be obtained by using experimental correlations. The mean velocity can also be obtained numerically, for example, by solving the Reynolds-average Navier-Stokes or boundary layer equations. Analytical correlations that were developed based on experimental data often consist of multiple functions for the different layers in turbulent boundary layers. The derivatives of the velocity are often discontinuous across these zones where different functional forms for the velocity profile are used. As the present eigenvalue problems are sensitive to the profile shapes of U and D^2U, the numerical solution of U and D^2U were used in the present calculations. In the results given here, these profiles were obtained by using dense grids ($\approx 1,000$) in a boundary-layer equation solver to retain a higher order of fidelity of the velocity as well as its second-order derivative. A mixing-length turbulence model was used for the turbulent eddy-viscosity.

Wavelike structure

To resolve the near-wall behavior of turbulent boundary layers, grids with constant stretching ratios were used in both the mean flow calculation and the wave calculations, equation (2) and (3). In the transformed coordinate, $\bar{y}$, the equations can be written as,

$$m(m(m(m\hat{v}')')')' + A_v m(m\hat{v}')' + B_v\hat{v} = 0 \tag{7}$$

$$m(m\hat{\eta}')' + B_\eta\hat{\eta} = 0, \tag{8}$$

where

$$A_v = -2(\alpha^2 + \beta^2) - \mathrm{i}Re(\alpha U - \omega)$$

$$B_v = (\alpha^2 + \beta^2)^2 + \mathrm{i}Re(\alpha^2 + \beta^2)(\alpha U - \omega) + \mathrm{i}Re\alpha D^2 U$$

$$B_\eta = -\mathrm{i}Re(\alpha U - \omega) - (\alpha^2 + \beta^2)$$

and

$$()' \equiv \frac{\mathrm{d}()}{\mathrm{d}\bar{y}}$$

$\bar{y}$ denotes the transformed coordinate. The transformation metric, m, is determined numerically. The global solution for the Orr-Sommerfeld and the vertical vorticity equations involves the use of second- and fourth-order accurate finite difference formulae for the equations and for the boundary conditions. The second-order formulae are widely available. The fourth order formulae used here are listed in the Appendix. The resulting homogeneous systems of equations form eigenvalue problems, for both the Orr-Sommerfeld and the vertical vorticity equations, nonlinear in the parameter, α. For the Orr-Sommerfeld equation the system can be written as

$$\mathbf{D_4}(\alpha)\mathbf{v} = 0 \tag{9}$$

The matrix, $\mathbf{D_4}$, is a lambda matrix of degree four (Lancaster, 1966), and can be expressed as a scalar polynomial with matrix coefficients:

$$\mathbf{D_4}(\alpha) = \mathbf{C_0}\alpha^4 + \mathbf{C_1}\alpha^3 + \mathbf{C_2}\alpha^2 + \mathbf{C_3}\alpha + \mathbf{C_4}. \tag{10}$$

With the inclusion of the boundary conditions, the matrices $\mathbf{C}'s$ are square matrices of order n, which represents the number of grid point in $\bar{y}$. A linear companion matrix method was used to linearize the lambda matrix. The resulting general eigenvalue problem becomes

$$\left\{\begin{pmatrix} -\mathbf{C_1} & -\mathbf{C_2} & -\mathbf{C_3} & -\mathbf{C_4} \\ \mathbf{I} & \mathbf{0} & \mathbf{0} & \mathbf{0} \\ \mathbf{0} & \mathbf{I} & \mathbf{0} & \mathbf{0} \\ \mathbf{0} & \mathbf{0} & \mathbf{I} & \mathbf{0} \end{pmatrix} - \alpha \begin{pmatrix} \mathbf{C_0} & \mathbf{0} & \mathbf{0} & \mathbf{0} \\ \mathbf{0} & \mathbf{I} & \mathbf{0} & \mathbf{0} \\ \mathbf{0} & \mathbf{0} & \mathbf{I} & \mathbf{0} \\ \mathbf{0} & \mathbf{0} & \mathbf{0} & \mathbf{I} \end{pmatrix}\right\} \begin{pmatrix} \alpha^3\hat{v} \\ \alpha^2\hat{v} \\ \alpha\hat{v} \\ \hat{v} \end{pmatrix} = \mathbf{0}. \tag{11}$$

Equation (11) can be further transformed to an algebraic eigenvalue problem seeking the eigenvalues of matrix $\mathbf{A}$:

$$\mathbf{A} = \begin{pmatrix} -\mathbf{C_0^{-1}C_1} & -\mathbf{C_0^{-1}C_2} & -\mathbf{C_0^{-1}C_3} & -\mathbf{C_0^{-1}C_4} \\ \mathbf{I} & \mathbf{0} & \mathbf{0} & \mathbf{0} \\ \mathbf{0} & \mathbf{I} & \mathbf{0} & \mathbf{0} \\ \mathbf{0} & \mathbf{0} & \mathbf{I} & \mathbf{0} \end{pmatrix}. \tag{12}$$

The eigenvalues may be obtained by using QR or QZ algorithms. The details of the formulation and the application of the linear companion matrix method can be found in Bridges and Morris (1984) and Liou and Morris (1992a). Similarly, for the vertical vorticity equation, the system of equations can be written as

$$\mathbf{D_2}(\alpha)\eta = 0.$$

The eigenvalues can be obtained by using the procedure described above.

The resonance in the stability problem occurs when there is a set of parameters(α, β, ω) for which the solutions of the Orr-Sommerfeld and the vertical vorticity equations exist for a given mean velocity distribution and a Reynolds number. To locate the resonance mode, we choose to solve the following equations:

$$\alpha_r^{OS}(\beta, \omega) - \alpha_r^{VV}(\beta, \omega) = 0 \tag{13a}$$

$$\alpha_i^{OS}(\beta, \omega) - \alpha_i^{VV}(\beta, \omega) = 0 \tag{13b}$$

where α_r and α_i denote the real and the imaginary parts of α. A subroutine in the IMSL package called NEQBF has been used to solve the system of equations.

Results

In this section the numerical solutions of the resonance problem obtained by using the high order finite difference global method are described. To validate the numerical procedure, a polynomial type of distribution was first used as the mean velocity profile. The profile

$$U(\frac{y}{\delta}) = 2(\frac{y}{\delta}) - 2(\frac{y}{\delta})^3 + (\frac{y}{\delta})^4$$

was often used as an approximation to the streamwise velocity of flat plate boundary layers. δ represents the boundary-layer thickness. The eigenvalues obtained by using the present global method with fourth-order formulae and 201 grid points were compared with those obtained by using the local shooting method. The comparisons are shown in Table I.

Figure 2 shows the calculated complex phase velocity for a plane mode, and $Re(\frac{U_\infty \delta}{\nu}) = 8,000$ and 10,000 for the vertical vorticity equation. The frequencies are 0.0122 and 0.1202 respectively. An analytical form of the continuous spectrum (Grosch and Salwen, 1978) was also included for comparison. For $Re = 10,000$, the two discrete Tollmien-Schlichiting instability modescan be clearly identified. For $Re = 8,000$, the discrete spectrum appears close to the continuous spectrum. For both cases the continuous spectra are well-resolved.

Numerical experiments were conducted to examine the effects of the order of the finite difference approximation, the number of grid points, and the location of the outer boundary of the computed domain. Second-, as well as fourth-, order approximations were applied to the differential equations and the boundary conditions. Figure 3 shows a result of the calculated complex phase velocity for a plane mode for the Orr-Sommerfeld equation using various finite differencing, numbers of grid point, and $(\frac{\nu}{\delta})_{max}$. The symbols represent the results for different calculated cases denoted by a-b-c, where [a] denotes the order of accuracy, [b] the

Table I.
Comaprison of the calculated eigenvalues, α

Re	ω	Equations	Present	Shooting
8,000	0.2354	Orr-Sommerfeld	(0.780864,-0.013533)	(0.781148,-0.01356)
10,000	0.1202	Vertical vorticity	(0.41512, 0.40891)	(0.415119, 0.408911)

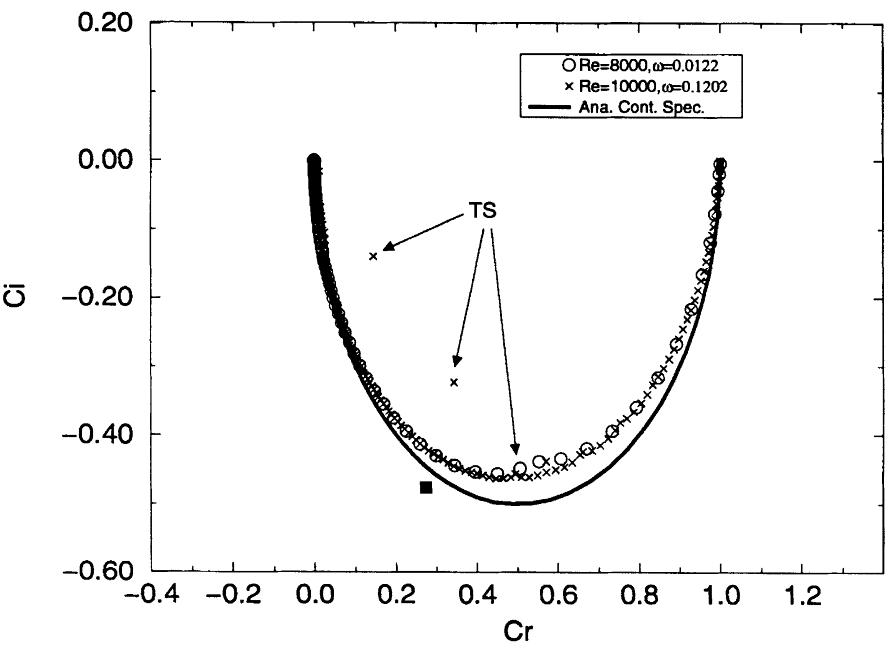

Figure 2.
Complex wave speed. Vertical vorticity equation

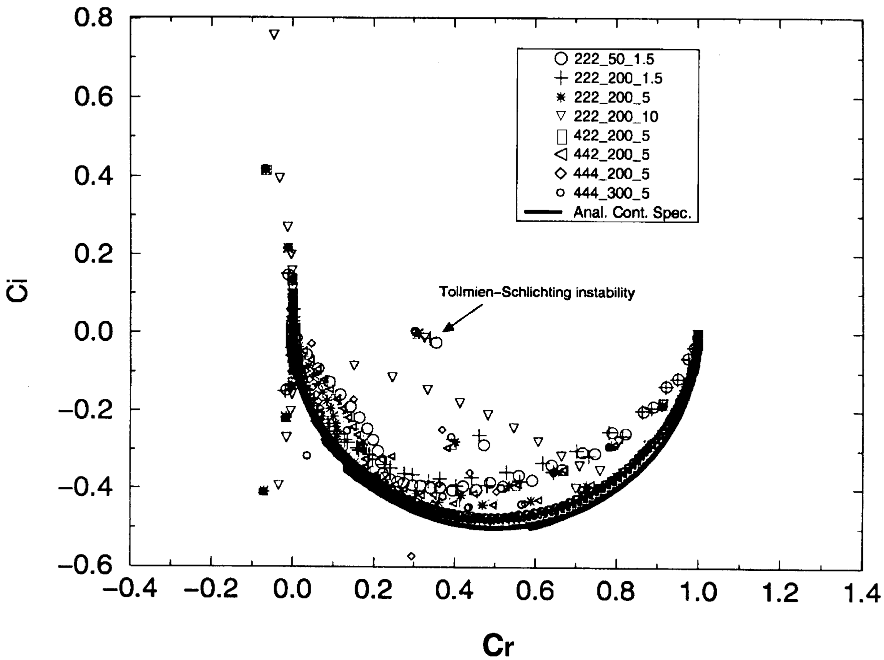

Figure 3. Comparison of eigenvalue spectra. Orr-Sommerfeld equation

number of discretized points used, and [c] the far field boundary distance to the wall. The first, second, and the third number in [a] represent the order of accuracy for the derivatives in the Orr-Sommerfeld equation, for the far field boundary conditions, and for the wall boundary conditions respectively. The agreement between the computed and the analytical continuous spectrum improves with the increasing number of grid nodes. It also appears that increasing the order of accuracy of the discretization enhances the agreement. Numerical experiments for the vertical vorticity equation yielded similar results. The results shown in the following for both the Orr-Sommerfeld and the vertical vorticity equations were obtained by using the fourth order formulae and a grid of 200 nodes.

To calculate the eigenvalues of the direct-resonant problems associated with a turbulent flat plate boundary layer, the mean streamwise velocity and its second derivative distribution were needed. A boundary-layer equation solver using the Prandtl's mixing length model with the van Driest damping function was developed. The calculated turbulent mean velocity distribution for $Re = 1,000$ is shown in Figure 4. The results compared well with the log law-of-the-wall in the log layer of the boundary layer. The number of grid points used is 998. The second derivative of the mean velocity, D^2U, was obtained using a fourth-order accurate finite difference formula. Figure 5 shows the D^2U distribution. For laminar boundary layers, the solutions of the Orr-Sommerfeld and vertical vorticity equations are known to be sensitive to the input velocity and its second derivative. We found that this sensitivity of the Orr-Sommerfeld and vertical vorticity equations to the input U and D^2U remains for the current problem

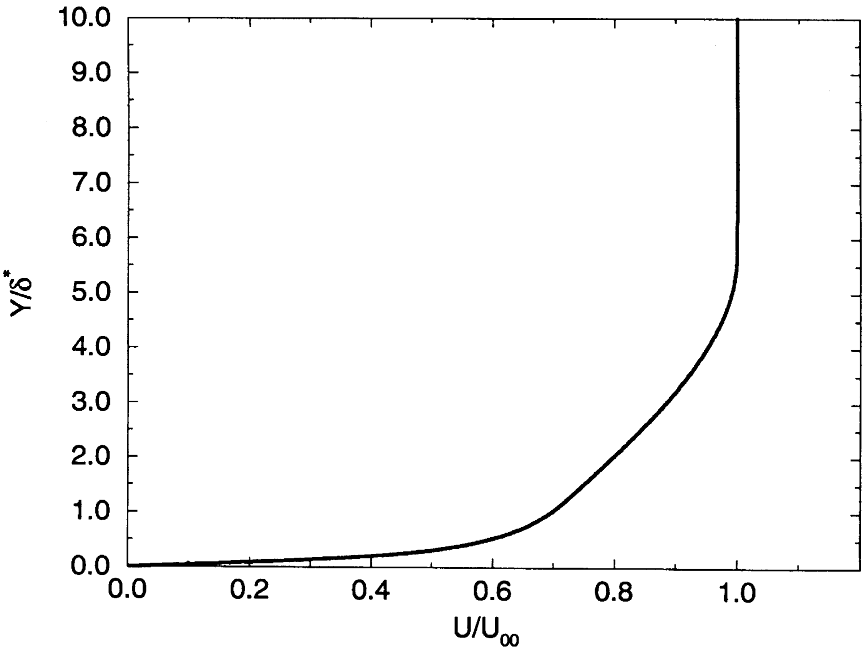

Figure 4. Streamwise mean velocity

involving turbulent boundary layers. As can be seen in Figures 4 and 5, the U and D^2U profiles vary significantly over a small distance in the near-wall region of the flow. It is necessary that the multiple length scales of turbulent boundary layers be resolved properly in the Orr-Sommerfeld and vertical vorticity problems. In this study, algebraically stretched grids were used to ensure an appropriate resolution of the mean flow. Comprehensive numerical experiments showed that a parameter set of $y_1^+ = 1$ and $(\frac{y}{\delta^*})_{max} = y_l = 50$ gives the best results in terms of both the discrete and the continuous spectra of the Orr-Sommerfeld and vertical vorticity equations for a wide range of Reynolds numbers. δ^* denotes the displacement thickness and $()_1$ the first grid point away from the wall. Figure 6 shows a typical result of the numerical experiments. Figure 6 shows the complex phase velocity spectrum of the vertical vorticity equation for $\omega = 2$; $\beta = 10$; $y_l = 50$; and $y_1^+ = 0.001, 0.01, 0.1, 1.0, 5.0$. Except for $y_1^+ = 5$, the computed discrete modes agree well. There is a more significant separation between the discrete and the continuous spectra for $y_1^+ = 1$ than for the other values. Similar results were also obtained for the Orr-Sommerfeld equation. This separation between the discrete and the continuous modes was used as a criterion to identify the discrete modes from the continuous modes in an automated procedure of bursting frequency prediction. A calculation with $y_1^+ = 1$ and $y_l = 90$ shows no changes in either the discrete or the continuous spectra. Figure 7 shows the eigenvalue spectrum for the Orr-Sommerfeld equation for a turbulent boundary layer for $Re(\frac{U_\infty \delta^*}{\nu}) = 1,000$.

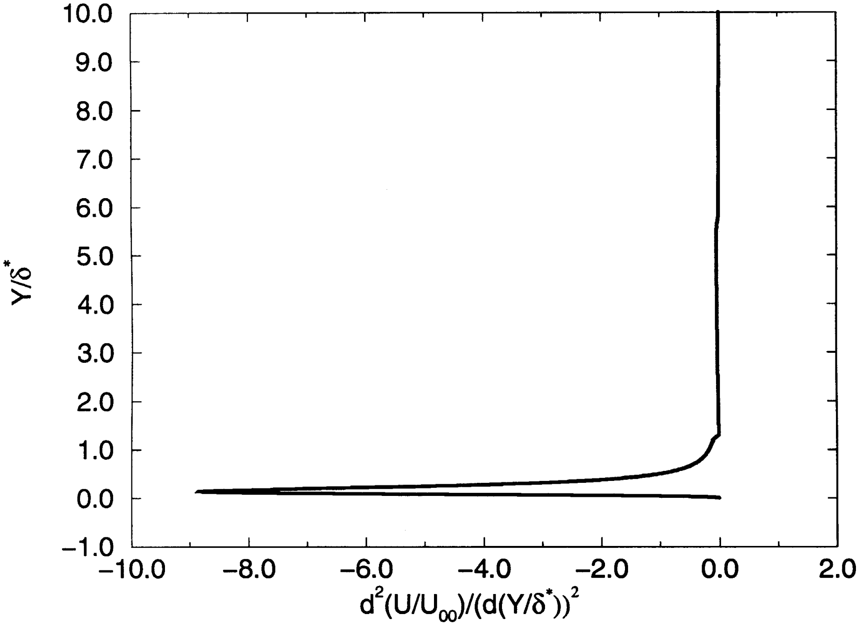

Figure 5.
Second order derivative of the mean velocity

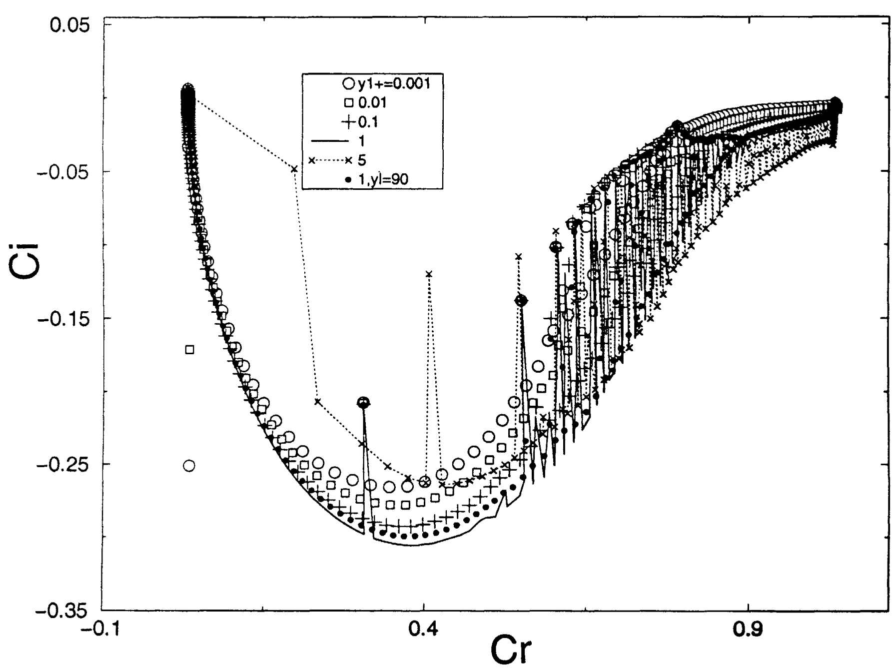

Figure 6.
Results of parametric studies. Vertical vorticity equation

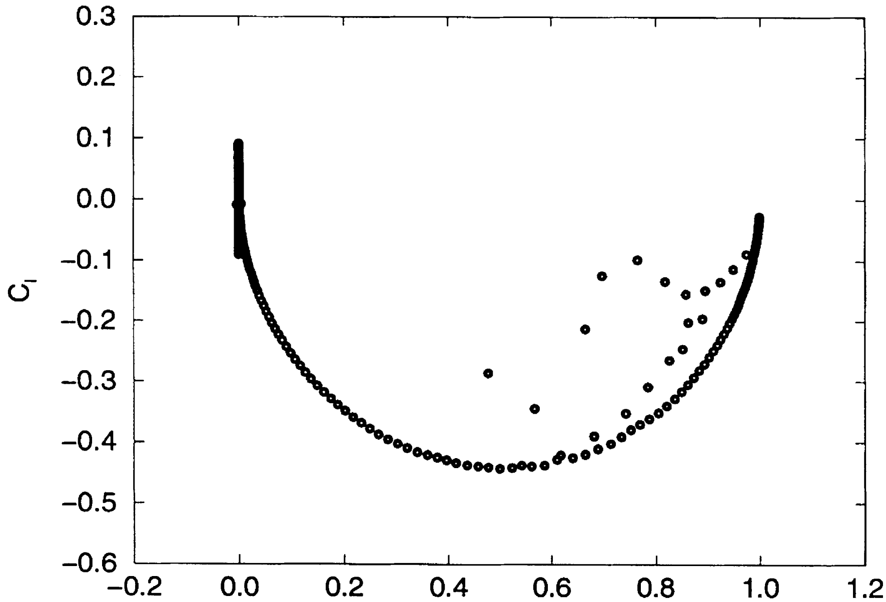

Figure 7.
Eigenvalue spectrum. Turbulent. Orr-Sommerfeld equation

As was stated earlier, based on the direct-resonance theory, an automated procedure has been developed for the prediction of the bursting frequencies associated with the streamwise structures in turbulent boundary layers. To identify a resonance mode, the Orr-Sommerfeld equation and the homogeneous vertical vorticity equation were first solved. Resonance occurs when the eigenvalues of the Orr-Sommerfeld solution correspond to that associated with the vertical vorticity equation. The resonance condition has been written in the form of a system of two equations, equation (13), nonlinear in their parameters, ω and β. The resonance mode is identified when a solution of Equation (13) is found. The solution of equation (13) involves an iteration process. The search for a resonance mode is complete when the solution of equation (13) is obtained. The procedure for searching the resonance mode has been automated. The automated search procedure was implemented in a FORTRAN software.

Figures 8, 9, and 10 show the results of using the automated procedure for a turbulent boundary layer of $Re = 1,000$. Figures 8 and 9 show the convergent history for the complex α and c respectively. The search process was terminated when the right-hand side of equation (13), denoted by d_R and d_I, have reduced to the order of –4. Figure 10 shows the evolution of d_R and d_I during an iteration process. The predicted resonant frequency is ω^+=0.0962, which compares well with that of Jang *et al.* (1986), of 0.09, calculated by using a shooting method for temporally developing turbulent boundary layers and the measured data by Morrison and Kronauer (1969).

The eigenvalue spectra for the Orr-Sommerfeld and vertical vorticity equations at the resonance condition for $Re = 8,000$ are shown in Figure 11.

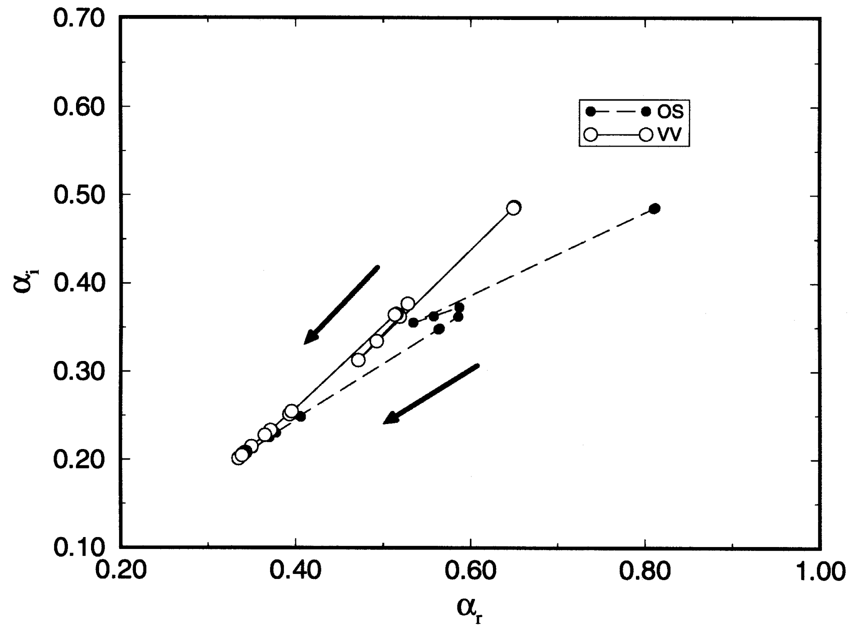

Figure 8.
Convergent history of α

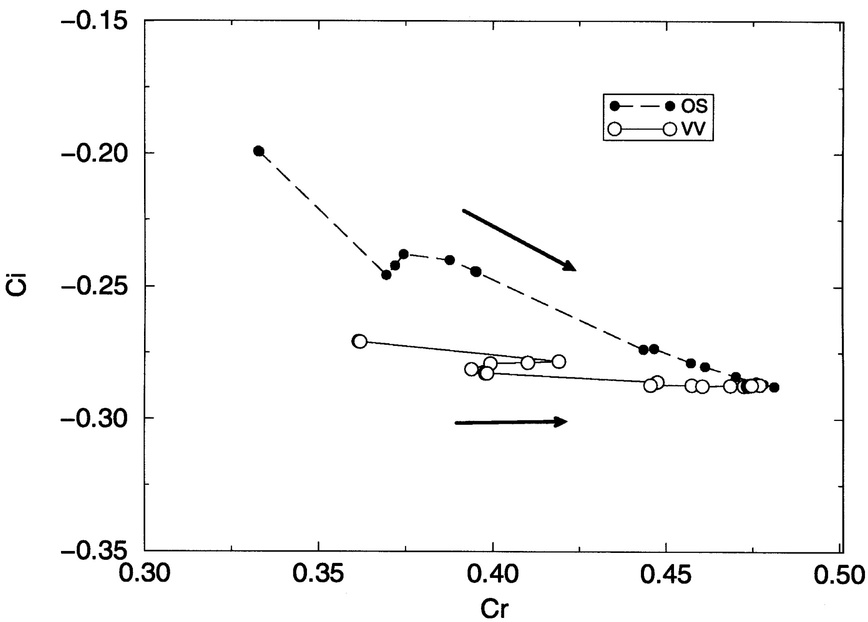

Figure 9.
Convergent history of c

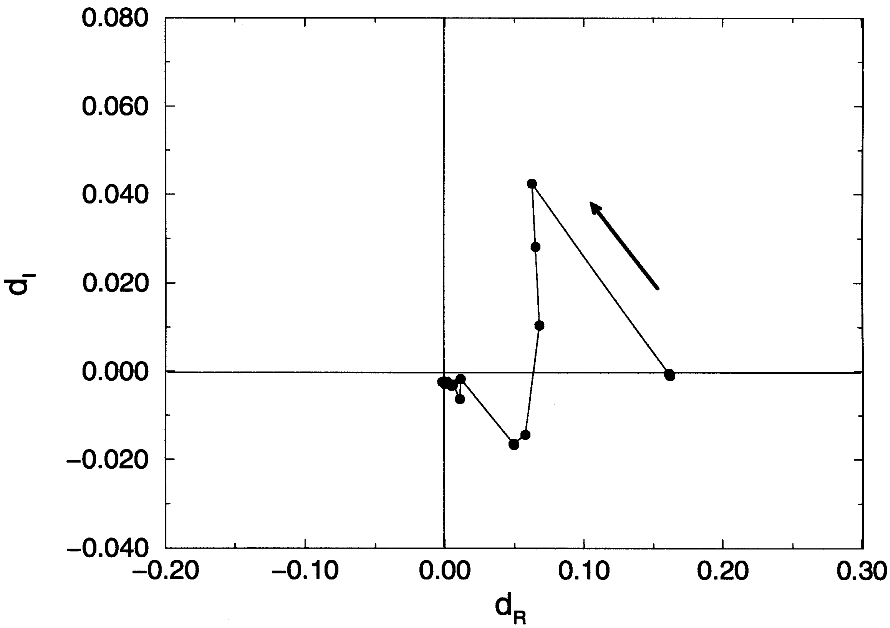

Figure 10.
Convergent history

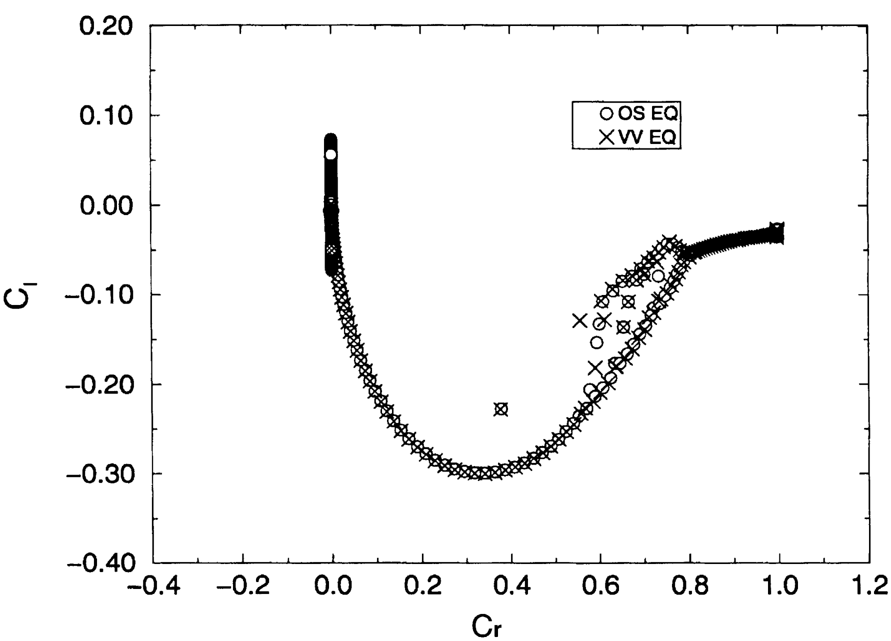

Figure 11.
Eigenvalue sprectrum at resonance. Re=8,000. Orr-Sommerfeld equation

The predicted resonance frequency was $\omega^+ = 0.0962$. Figure 11 also shows that, when the resonance condition is met, there is apparently a matching of not only the discrete mode but also the continuous modes.

Concluding remarks

In this study a global solution method has been successfully developed to predict the bursting frequencies associated with the coherent streamwise structures in incompressible turbulent boundary layers. The prediction was based on the direct resonance model. The prediction tool developed has been automated, and no artificial intervention is necessary other than assigning the starting values. In the present study the predicted bursting frequencies have been found to agree very well with previous numerical calculations and experimental data for incompressible turbulent boundary layers over a flat plate.

References

Baty, R.S. and Morris, P.J. (1995), "The instability of jets of arbitrary exit geometry", *International Journal of Numerical Methods in Fluids*, Vol. 21 p. 763.

Bridges, T.J. and Morris, P.J. (1984), "Differential eigenvalue problems in which the parameter appears nonlinearly", *Journal of Computational Physics*, Vol. 55 p. 437.

Cantwell, B.J. (1989), "Future directions in turbulence research and the role of organized motion", Whither Turbulence Workshop, Cornell University.

Grosch, C.E. and Salwen, H. (1978), "The continuous spectrum of the Orr-Sommerfeld equation. Part I. The spectrum and the eigenfunctions", *Journal of Fluid Mechanics*, Vol. 87 p. 33.

Jang, P.S., Benny, D.J. and Gran, R.L. (1986), "On the origin of streamwise vortices in a turbulent boundary layer", *Journal of Fluid Mechanics*, Vol. 169 p. 109.

Lancaster, P. (1966), *Lambda Matrices and Vibrating Systems*, Permagon, Oxford.

Liou, W.W. and Morris, P.J. (1992a), "The eigenvalue spectrum of the Rayleigh equation for a plane shear layer", *International Journal of Numerical Methods in Fluids*, Vol. 15 p. 1407.

Liou, W.W. and Morris, P.J. (1992b), "Weakly nonlinear models for turbulent mixing in a plane mixing layer", *Physics of Fluids*, Vol. 4 p. 2798.

Morrison, W.R.B. and Kronauer, R.E. (1969), "Structural similarity for fully developed turbulence in smooth tubes", *Journal of Fluid Mechanics*, Vol. 39 p. 117.

Appendix

The fourth order, $O(\Delta^4)$, finite difference formulae used in the current study are given below. All formulae are given for the derivatives at a point denoted by $()_0$ and its neighboring points in decreasing order, $()_{-1}$, $()_{-2}$,..., and in increasing order, $()_{+1}$, $()_{+2}$,..., etc.. Δ denotes the uniform grid spacing.

$$f_0' = \frac{f_{-2} - 8f_{-1} + 8f_1 - f_2}{12\Delta}$$

$$f_0' = \frac{-3f_{-1} - 10f_0 + 18f_1 - 6f_2 + f_3}{12\Delta}$$

$$f_0' = \frac{3f_1 + 10f_0 - 18f_{-1} + 6f_{-2} - f_{-3}}{12\Delta}$$

HFF
10,8

$$f_0' = \frac{-25f_0 + 48f_1 - 36f_2 + 16f_3 - 3f_4}{12\Delta}$$

$$f_0' = \frac{25f_0 - 48f_{-1} + 36f_{-2} - 16f_{-3} + 3f_{-4}}{12\Delta}$$

$$f_0'' = \frac{-2f_{-2} + 16f_{-1} - 30f_0 + 16f_1 - f_2}{12\Delta^2}$$

$$f_0'' = \frac{10f_{-1} - 15f_0 - 4f_1 + 14f_2 - 6f_3 + f_4}{12\Delta^2}$$

$$f_0'' = \frac{10f_1 - 15f_0 - 4f_{-1} + 14f_{-2} - 6f_{-3} + f_{-4}}{12\Delta^2}$$

$$f_0''' = \frac{f_{-3} - 8f_{-2} + 13f_{-1} - 13f_1 + 8f_2 - f_3}{8\Delta^3}$$

$$f_0''' = \frac{-f_{-2} - 8f_{-1}35f_0 - 48f_1 + 29f_2 - 8f_3 + f_4}{8\Delta^3}$$

$$f_0''' = \frac{f_2 + 8f_1 - 35f_0 + 48f_{-1} - 29f_{-2} + 8f_{-3} - f_{-4}}{8\Delta^3}$$

$$f_0'''' = \frac{-f_{-3} + 12f_{-2} - 39f_{-1} + 56f_0 - 39f_1 + 12f_2 - f_3}{6\Delta^4}$$

$$f_0'''' = \frac{20f_{-2} - 55f_{-1} + 155f_1 - 220f_2 + 135f_3 - 40f_4 + 5f_5}{30\Delta^4}$$

$$f_0'''' = \frac{20f_2 - 55f_1 + 155f_{-1} - 220f_{-2} + 135f_{-3} - 40f_{-4} + 5f_{-5}}{30\Delta^4}$$